THE JOURNAL OF PHYSICAL CHEMISTRY A
A JOURNAL OF THE AMERICAN CHEMICAL SOCIETY

pubs.acs.org/JPCA

Article

Second-Order Kinetic Rate Coefficients for the Aqueous-Phase Sulfate Radical ($SO_4^{\bullet-}$) Oxidation of Some Atmospherically Relevant Organic Compounds

Published as part of The Journal of Physical Chemistry virtual special issue "Advances in Atmospheric Chemical and Physical Processes".

Lillian N. Tran, Karizza A. Abellar, James D. Cope, and Tran B. Nguyen*

Cite This: *J. Phys. Chem. A* 2022, 126, 6517−6525

Read Online

ACCESS | Metrics & More | Article Recommendations | Supporting Information

ABSTRACT: The sulfate anion radical ($SO_4^{\bullet-}$) is a reactive oxidant formed in the autoxidation chain of sulfur dioxide, among other sources. Recently, new formation pathways toward $SO_4^{\bullet-}$ and other reactive sulfur species have been reported. This work investigated the second-order rate coefficients for the aqueous $SO_4^{\bullet-}$ oxidation of the following important organic aerosol compounds (k_{SO4}): 2-methyltetrol, 2-methyl-1,2,3-trihydroxy-4-sulfate, 2-methyl-1,2-dihydroxy-3-sulfate, 1,2-dihydroxyisoprene, 2-methyl-2,3-dihydroxy-1,4-dinitrate, 2-methyl-1,2,4-trihydroxy-3-nitrate, 2-methylglyceric acid, 2-methylglycerate, lactic acid, lactate, pyruvic acid, pyruvate. The rate coefficients of the unknowns were determined against that of a reference in pure water in a temperature range of 298−322 K. The decays of each reagent were measured with nuclear magnetic resonance (NMR) and high-performance liquid chromatography−high-resolution mass spectrometry (HPLC-HRMS). Incorporating additional $SO_4^{\bullet-}$ reactions into models may aid in the understanding of organosulfate formation, radical propagation, and aerosol mass sinks.

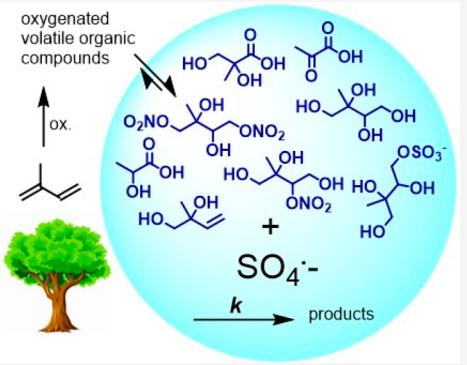

INTRODUCTION

A wide variety of water-soluble condensed-phase compounds are formed during the oxidation of reactive carbon emissions in the atmosphere.[1−3] The oxidation of reactive carbon emissions in the aqueous phases of aerosols, fogs, and clouds initiated by hydroxyl (OH) radicals, nitrate (NO_3) radicals, and the sulfate anion radical ($SO_4^{\bullet-}$) has been reviewed previously (refs 4−6 and references therein). $SO_4^{\bullet-}$ radicals have been recognized as a potentially important source of surface-active organosulfates (OSs) in the environment,[7−10] which can modify aerosol cloud interactions.[11,12] A large variety of OSs have been identified in both field and laboratory studies, several of which are proposed to only be formed from $SO_4^{\bullet-}$ radicals.[9,13−17] The $SO_4^{\bullet-}$ radical is thought to be formed primarily in the autoxidation of SO_2; however, it can also be formed from the activation of sulfate and bisulfate anions with OH, NO_3,[4] and to a small extent ferric ion complexes.[18,19] Although the atmospheric concentration of the $SO_4^{\bullet-}$ radical has not been directly measured, it has been estimated between 9.1×10^{-13} and 5.5×10^{-17} M, assuming known sources.[4] New mechanisms of reactive sulfur species relevant to sulfate aerosols have been recently reported, including $SO_4^{\bullet-}$ formation from irradiated sulfate aerosols,[20] OH-initiated oxidation of organosulfates,[21] and autocatalysis of the SO_4^{2-} anion in the presence of phenols.[22] The formation of reactive sulfur was also reported from the interfacial redox of ammonium sulfate aerosol particles.[23] Thus, the chemistry and environmental source calculations of $SO_4^{\bullet-}$ and other sulfur radicals may benefit from re-evaluation in models.

With this in mind, chemical transport models need second-order $SO_4^{\bullet-}$ rate coefficients (k_{SO4}) for water-soluble organic compounds to better represent condensed-phase chemistry. However, k_{SO4} rate coefficients for complex compounds present in biogenic organic aerosols are largely unknown.[5,24−26] As these compounds may contain a diverse array of functional groups, effort may be required to synthesize and purify them, and a multitude of instrumental methods are required for their analysis. Previously, we reported the second-order rate coefficients for aqueous hydroxyl radical (OH) oxidation (k_{OH}) for several oxidation products of isoprene obtained through chemical synthesis, which were measured using competitive rate experiments with erythritol.[27] We follow

Received: July 13, 2022
Revised: August 30, 2022
Published: September 7, 2022

https://doi.org/10.1021/acs.jpca.2c04964
J. Phys. Chem. A 2022, 126, 6517−6525

up here with their k_{SO4} rates and add some additional organic acids to the study. Detailed justifications for the study of the isoprene-related species were presented in-depth previously, along with the synthetic and analytical method development. Briefly, the isoprene-derived compounds under study are either formed from the gas-phase oxidation of isoprene[1] and partitioned to the condensed phase due to their low vapor pressure or formed after a multiphase reaction (Scheme 1A).

Scheme 1. (A) Compounds Originating from Isoprene, (B) a Structural Analog to Isoprene's Organosulfate, and (C) Compounds Originating from Various and Often Multiple Sources in the Atmosphere[a]

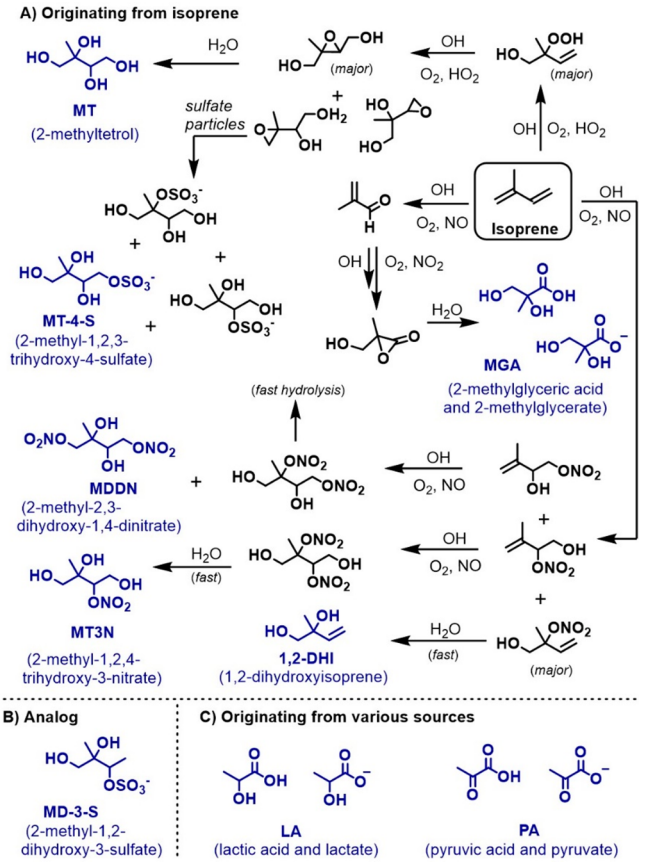

[a]Compounds under study are shown in blue. The isoprene scheme is derived from Wennberg et al.[1]

these compounds include products from the low-NO channel, including 2-methyltetrol (MT) and 2-methyl-1,2,3-trihydroxy-4-sulfate (MT-4-S),[28−32] and from the high-NO channel, including 2-methyl-2,3-diol-1,4-dinitrate (MD-1,4-DN), 2-methyl-1,2,4-triol-3-nitrate (MT-3-N),[33] 1,2-dihydroxyisoprene (1,2-DHI, referred to as MDE in our previous work)[39−41] and 2-methylglyceric acid (MGA).[34,35] A structural analog of isoprene's organosulfate, 2-methyl-1,2-dihydroxy-3-sulfate (MD-3-S), was obtained as a side product in the chemical synthesis of MT-4-S and studied here to gain insight into the structural reactivity. In this work, we also examine some small organic acids such as lactic acid (LA) and pyruvic acid (PA) because they are ubiquitous in the atmospheric condensed phase.[36]

METHODS

Materials and Synthesis. Erythritol (99%), xylitol (≥99%), potassium persulfate ($K_2S_2O_8$, 99%), acetonitrile (99%), and pyruvic acid (≥99%) were obtained from Sigma-Aldrich. α-Methylglyceric acid (M311505, 98%) was purchased from Toronto Research Chemical s (TRC), Inc. Formic acid (≥99%) was purchased from Thermofisher Scientific. Lactic acid (90% in water) was purchased from Acros Chemicals. All reagents were used without further purification. Compounds were dissolved and diluted using ultrapure H_2O from a Milli-Q purification system (Millipore Sigma, 18 MΩ cm^{-1}). 2-Methyltetrol (MT), 1,2-dihyroxyisoprene (1,2-DHI), 2-methyl-1,2,3-trihydroxy-4-sulfate (MT-4-S), and 2-methyl-1,2-dihydroxy-3-sulfate anion (MD-3-S) were synthesized and purified according to the literature;[37] their nuclear magnetic resonance (NMR) spectra matched previously reported data. The organosulfates were purified for use over an ion-exchange column (Dowex 50WX4, 50−100 mesh). 2-Methyl-2,3-dihydroxy-1,4-dinitrate (MD-1,4-DN) and 2-methyl-1,2,4-trihydroxy-3-nitrate (MT-3-N) were synthesized previously by our group.[27] All synthesized chemicals used in this work had purities >95%, as determined by ^{1}H NMR. Due to the relative rate technique and the accurate-mass or structure-specific analytical measurements, organic impurities are not expected to alter the reaction kinetic ratios.

Experiments. Photochemical reactions of organic compounds of interest with sulfate radicals were examined in quartz reaction vessels using the UV irradiation of potassium persulfate ($K_2S_2O_8$) as a sulfate radical precursor. Similarly to other studies, the stable reactant was used in large excess relative to $SO_4^{\bullet-}$ in order to ensure pseudo steady-state kinetics.[38]

$$S_2O_{8^{2-}} + h\nu \rightarrow 2SO_4^{\bullet-} \quad \text{(i)}$$

$$SO_4^{\bullet-} + H_2O \rightarrow OH^{\bullet} + HSO_4^- \quad \text{(ii)}$$

$$2SO_4^{\bullet-} \rightarrow S_2O_8^{2-} \quad \text{(iii)}$$

A relative rate technique[39] was used, where the second-order rate coefficients for the compound of interest with respect to oxidation by the $SO_4^{\bullet-}$ radical were determined against a reference compound with a known rate coefficient in the same reaction. The reference compound selected for study was erythritol ($C_4H_{10}O_4$), which has a rate constant of 4.56×10^7 M^{-1} s^{-1} with the sulfate radical when averaged over the experimental temperature range.[24,40]

$$SO_4^{\bullet-} + \text{compound of interest} \rightarrow \text{products} \quad (1)$$

$$SO_4^{\bullet-} + \text{erythritol} \rightarrow \text{products} \quad (2)$$

Under the conditions of our study, J_i is $\sim 5.5 \times 10^{-5}$ s^{-1}. Using known rate coefficients for the above reactions (e.g., k_{ii} $\sim$ 400 s^{-1})[41] and those of erythritol with OH and $SO_4^{\bullet-}$,[4] it was estimated that >99% of the reaction proceeded via $SO_4^{\bullet-}$ compared to OH (Table S1).

Rate coefficients for the reactions were obtained as follows:

$$\ln\left(\frac{[\text{compound of interest}]_0}{[\text{compound of interest}]_t}\right) = \frac{k_1}{k_2}\ln\left(\frac{[\text{erythritol}]_0}{[\text{erythritol}]_t}\right)$$

where $[\text{compound of interest}]_0$ and $[\text{erythritol}]_0$ are the respective chromatographic or spectroscopic peak areas for those species at time zero, $[\text{compound of interest}]_t$ and

https://doi.org/10.1021/acs.jpca.2c04964
J. Phys. Chem. A 2022, 126, 6517−6525

$[\text{erythritol}]_t$ are the peak areas at time t, and k_1 and k_2 are the bimolecular rate coefficients for reactions 1 and 2, respectively. Plotting $\ln([\text{erythritol}]_0/[\text{erythritol}]_t)$ and $\ln([\text{compound of interest}]_0/[\text{compound of interest}]_t)$ generates a linear plot in the positive quadrant, where k_1/k_2 is the slope of the line.

Solutions of 5 mM erythritol, 15−20 mM $K_2S_2O_8$, and 5 mM compound of interest were prepared in Milli-Q water for experiments. The unadjusted pH values for MGA, PA, and LA were 3, 5, and 2, respectively. To analyze 2-methylglycerate and lactate (pH 5), NaOH was added dropwise to the mixed solution until pH 5 was reached. MGA and pyruvic acid were analyzed at pH 2 by adding H_2SO_4 dropwise to the mixed solution until pH 2 was reached. All other determinations were performed at pH 5−7. A quartz reaction vessel was filled with 10−15 mL of the sample mixture, placed in an enclosed compartment with a 254 nm UV lamp, and irradiated over the course of two hours (See Figure 1 for the experimental setup).

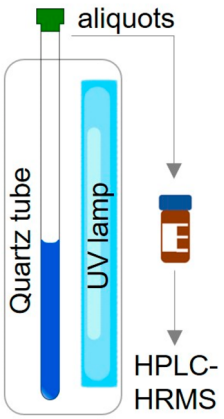

Figure 1. Experimental set-up. A quartz reaction tube within a glass compartment is exposed to a UV lamp. Aliquots of the sample at different time points are diluted and analyzed via HPLC-HRMS.

Using 400 μL H_2O spiked with xylitol (0.762 mM) as an internal standard, 100 μL aliquots of the reaction solution were analyzed at variable time points after dilution. Representative data are shown in Figure 2. All experiments were performed in triplicate, and uncertainty bounds represent one standard deviation.

Direct photolysis controls for compounds with chromophoric functional groups were performed identically to the experiment except without the erythritol reference and without $K_2S_2O_8$. The spectral output from the lamp was measured using a portable spectrophotometer (Tidas series, WPI Inc.), and the photo flux (Figure 3A) was calibrated using the neutral aqueous photolysis of uridine as a chemical actinometer according to protocol L09 from IUPAC.[42] Erythritol and other compounds without chromophores are assumed to undergo negligible photolysis during the experiment. A first-order loss rate (J) was extracted from the control experiments for the compounds of interest, and a correction to the raw data was performed where the k_1/k_2 ratio was obtained by plotting $\ln([\text{erythritol}]_0/[\text{erythritol}]_t)$ against $\ln([\text{compound of interest}]_0/[\text{compound of interest}]_t - J \times t)$. For experiments with photolysis controls, the uncertainties in the J determinations (e.g., errors in slopes) were propagated together with the standard deviations from the data.

In order to understand the temperature fluctuations during an experiment, a control experiment with Milli-Q water was

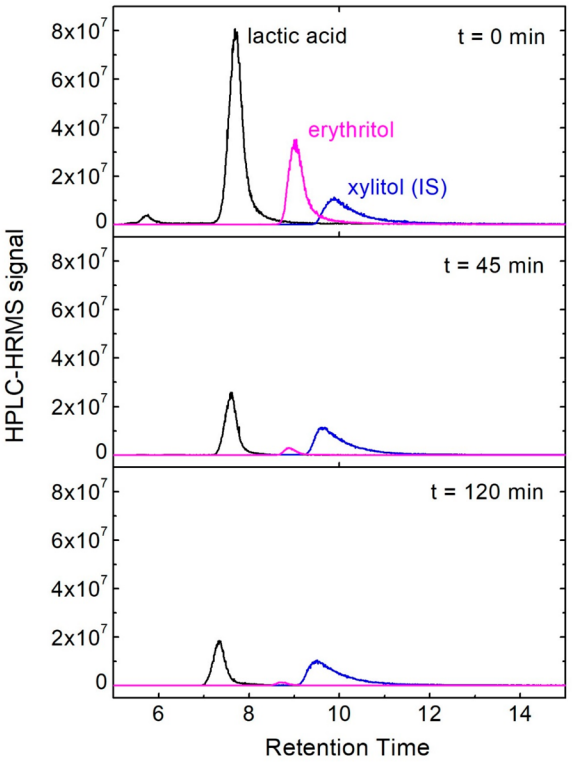

Figure 2. Representative HPLC-HRMS data for a kinetics experiment using lactic acid against erythritol at pH 2. Xylitol was added as an internal standard (IS). Data are normalized to the IS peak area.

performed with continuous irradiation while the temperature was monitored with a thermocouple (Figure S1). The temperature of the solution was recorded until temperature stabilization occurred. Thus, data are reported in the range of 298−322 K. The studied compounds are stable at these temperatures. Although the kinetic data are referenced and $SO_4^{\bullet-}$ reaction rates with similar compounds are weakly dependent on temperature,[26,40] it is not clear whether the temperature dependence of the rate coefficient for the reference compound is identical to that of the compound of interest. Partitioning to the gas phase may increase at higher temperatures in the capped quartz tube; however, all studied compounds have large Henry's Law coefficients that favor the aqueous phase by many orders of magnitude. 1,2-DHI is likely the most volatile compound in the study; its Henry's law coefficient may be estimated based on 1,2-pentanediol (K_H = 1.4 × 10^5 M atm^{-1} or 3.4 × 10^6 mole ratio of aqueous to gas).[43] The temperature uncertainty can be considered a limitation of this work.

Analytical Measurements. All analytes, with the exception of 1,2-DHI, were analyzed using high-performance liquid chromatography (HPLC) coupled to high-resolution mass spectrometry (HRMS). The HPLC-HRMS analyses were performed using an Agilent 1100 HPLC coupled to a linear-trap-quadrupole Orbitrap (LTQ-Orbitrap) mass spectrometer (Thermo Corp., Waltham MA) operated at a mass resolving power of 60 000 m/Δm at m/z 400. Xcalibur 2.0 software was used to analyze the mass spectra. The separation of MT, MD-1,4-DN, MT-3-N, erythritol, and xylitol was performed using a Shodex Asahipak NH2P-40 2D column (2 × 150 mm, 4 μm, 100 Å) using a method recently reported elsewhere.[27] An Agilent Poroshell InfinityLab EC-C18 (2.1 × 100 mm, 2.7 μm,

https://doi.org/10.1021/acs.jpca.2c04964
J. Phys. Chem. A 2022, 126, 6517−6525

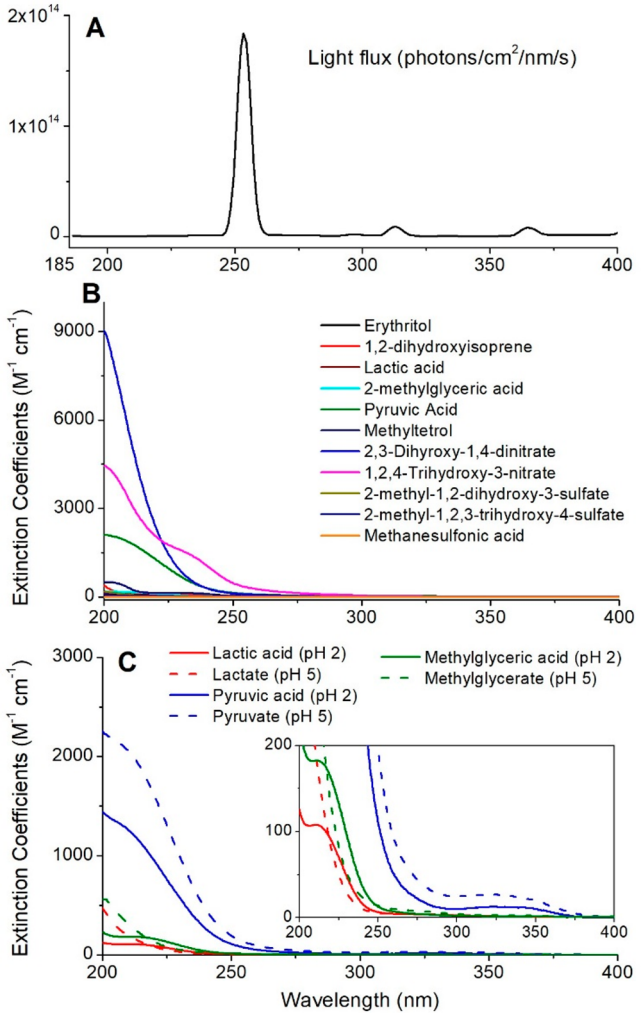

Figure 3. (A) Wavelength-dependent photon flux from the UV lamp, which was calibrated using chemical actinometry. Optical extinction coefficients (M^{-1} cm^{-1}) for (B) all compounds under study in pure water at unadjusted pH and (C) for the carboxylic acids at two pH values. The insert in panel C shows a magnified view of the absorbance features of organic acids in the 200−400 nm region.

120 Å) column was used to separate MD-3-S and MT-4-S using a previously reported method.[27] To analyze pyruvic acid, lactic acid, and MGA, including erythritol and xylitol, a Shodex HILICpak VG-50 2D column (2 × 150 mm,5 μm, 100 Å) was used. The mobile phases were MeCN (A) and 0.5% NH_3 (B), and the injection volume was 1 μL. To separate MGA from erythritol and xylitol, the mobile phase was held at 30% B for 2 min, increased to 90% B for 10 min, held at 90% for 3 min, decreased to 30% for 5 min, and held at 30% for another 5 min. The flow rate was 0.3 mL min^{-1}, and the total run time was 25 min. To separate pyruvic acid and lactic acid from erythritol and xylitol, the mobile phase was held at 30% B for 4 min, increased to 90% for 6 min, held at 90% for 1 min, decreased to 30% for 4 min, and held at 30% for 2 min. The flow rate was 0.1 mL min^{-1}, and the total run time was 17 min. A representative HPLC-HRMS data set for lactic acid is shown in Figure 2.

For the rate determinations of 1,2-DHI, proton nuclear magnetic resonance (^{1}H NMR) spectroscopy was used to quantify the decay of erythritol and 1,2-DHI due to the distinct proton environments of the alkene using a method similar to that we reported previously.[27] 1,2-DHI is poorly ionizable in the HPLC-HRMS method. Due to the lower sensitivity of the NMR analysis, 100 mM concentrations of both reactants were mixed with 300 mM $K_2S_2O_8$ in order to increase the analytical signal. Reactions for NMR analyses were performed on a 400 MHz Bruker instrument (400 MHz Bruker Avance III HD Nanobay Spectrometer) using an autosampler and analyzed using TOPSPIN. The solution was irradiated over the course of 1.5 h and taken to the instrument without any workup at several time points.

A Shimadzu UV-1800 dual-beam spectrophotometer was used to measure the UV−visible extinction coefficients of organic reactants as referenced with pure water, primarily to assess which reactant required a direct photolysis correction. A 1 cm quartz cuvette was used for the absorbance measurements for 0.1−1 mM samples, which were diluted in order to maintain Beer's Law linearity when required. Extinction coefficients were then calculated based on the measured absorbances, the path length, and the known concentrations of the solution.

RESULTS AND DISCUSSION

Direct Photolysis. It was found that pyruvic acid (PA, pH 2 and pH 5), 1,2-DHI, MD-1,4-DN, and MT-3-N had non-negligible absorption cross sections (>20 M^{-1} cm^{-1}) at 254 nm (Figure 3) that required a direct photolysis correction. A magnified view of Figure 3B is shown in Figure S2. These compounds have chromophores such as carbonyl, alkenyl, and nitrato groups, so their absorbance in the 200−400 nm range is expected. Pyruvic acid has a carbonyl in the β-position relative to the acid, which increases its chromophoric properties compared to those of hydroxyacids such as lactic acid. Photolysis controls performed for these compounds (Figure S3) yielded first-order loss rates of approximately 5−40 × 10^{-5} s^{-1}, which were used to correct the rate ratios against erythritol. Quantum yields under our lamp could be estimated to be in the range of ∼0.1−0.2 for the organonitrates and pyruvate (pH 5) but were larger than unity for pyruvic acid (PA) and 1,2-DHI (Table S2). Eugene et al.[44] reported that the photolytic loss of PA in water at pH 1 proceeds with a quantum yield of ∼2, in good agreement with our estimate (2.4). Effectively, each PA* molecule that is excited per absorbed photon consumes another molecule of PA in a highly efficient bimolecular process. Although the chromophore-loss quantum yield of pyruvate in water has not been reported, to our knowledge, the decarboxylation quantum yield for pyruvate is at least twenty times smaller than that for the acid,[45] in qualitative agreement with the much smaller quantum yield we extracted for pyruvate loss (0.19). Aqueous photolysis data for other compounds studied in this work were not available in the literature for further comparisons.

Kinetics Experiments. From the decay of erythritol, the steady-state concentrations of $SO_4^{\bullet-}$ used for experiments were determined in the range of 0.1−2 × 10^{-11} M. Ratios of k_1/k_2 for the different compounds of interest, derived from triplicate trials, are shown in Figures 4 and 5. Data points were fit linearly, with the slope being "k_1/k_2". Direct photolysis corrections are shown in blue where appropriate. Table 1 shows the k_{SO4} values for the compounds under study after the application of the rate coefficient of erythritol to the respective rate ratios. Control experiments did not show appreciable reactions between organics and the $K_2S_2O_8$ reagent in the dark

https://doi.org/10.1021/acs.jpca.2c04964
J. Phys. Chem. A 2022, 126, 6517−6525

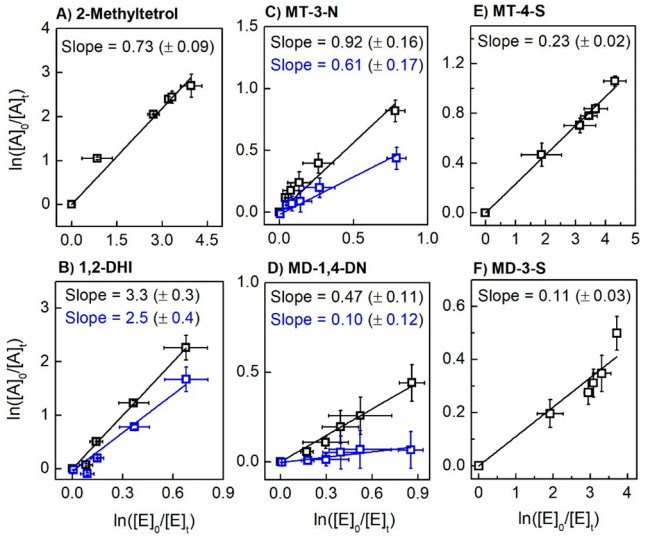

Figure 4. Relative rate determinations for the isoprene-derived polyols, organonitrates, and organosulfates ("A") against reference erythritol ("E"). Data shown in blue are corrected for direct photolysis. (A) 2-Methyltetrol, (B) 1,2-dihydroxyisoprene (1,2-DHI), (C) 2-methyl-1,2,4-trihydroxy-3-nitrate (MT-3-N), (D) 2-methyl-2,3-dihydroxy-1,4-dinitrate (MD-1,4-DN), (E) 2-methyl-1,2,3-trihydroxy-4-sulfate (MT-4-S), and (F) 2-methyl-1,2-dihydroxy-3-sulfate (MD-3-S). A linear least-squares fit assumes a *y*-intercept of zero. Chemical structures are shown in Scheme 1.

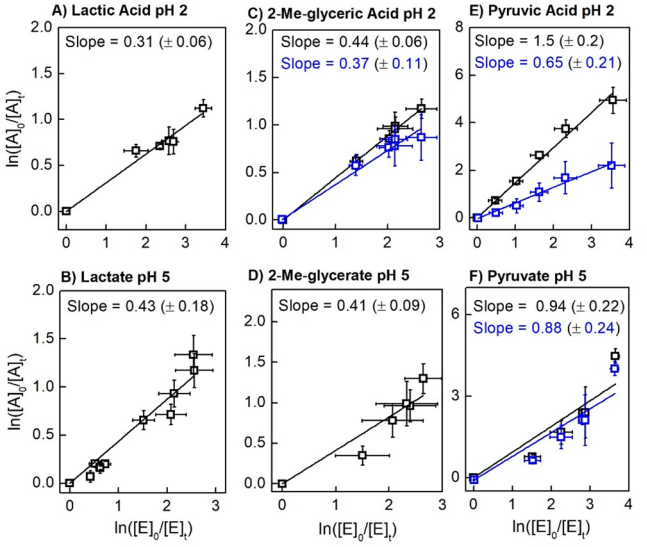

Figure 5. Relative rate determinations for carboxylic acid compounds of interest and their carboxylates ("A") against reference compound erythritol ("E"). (A) Lactic acid, (B) lactate, (C) 2-methylglyceric acid, (D) 2-methylglycerate, (E) pyruvic acid, and (F) pyruvate. Data shown in blue are corrected for direct photolysis. A linear least-squares fit assumes a *y*-intercept of zero. Chemical structures are shown in Scheme 1.

at the concentrations and time scales relevant to this work (Figure S4).

Starting with the isoprene-derived polyols, organonitrates, and organosulfates (Figure 4), we see the largest rate coefficient in the reaction of 1,2-DHI versus erythritol. The unsaturation in 1,2-DHI enables an addition mechanism for $SO_4^{\bullet-}$ that is unavailable for the other compounds under study

Table 1. Measured Second-Order k_{SO4} Rate Coefficients in Water in the Range of 298−322 K[a]

compound	abbreviation	k_{SO4} (M^{-1} s^{-1})[b]
2-methyltetrol	MT	3.3 (±0.4) × 10^7
2-methyl-2,3-dihydroxy-1,4-dinitrate	MD-1,4-DN	4.6 (±5.0) × 10^6
2-methyl-1,2,4-trihydroxy-3-nitrate	MT-3-N	2.8 (±0.7) × 10^7
1,2-dihydroxyisoprene	1,2-DHI	1.1 (±0.2) × 10^8
2-methyl-1,2,3-trihydroxy-4-sulfate	MT-4-S	1.1 (±0.8) × 10^7
2-methyl-1,2-dihydroxy-3-sulfate	MD-3-S	5.0 (±1.3) × 10^6
2-methylglyceric acid	MGA (pH 2)	1.7 (±0.5) × 10^7
	MGA (pH 5)	1.9 (±0.4) × 10^7
Lactic acid	LA (pH 2)	1.4 (±0.3) × 10^7
	LA (pH 5)	2.0 (±0.8) × 10^7
Pyruvic acid	PA (pH 2)	3.0 (±0.9) × 10^7
	PA (pH 5)	4.0 (±1.4) × 10^7

[a]Direct photolysis corrections have been applied, where appropriate. Chemical structures are shown in Scheme 1. [b]Measured against reference compound erythritol (4.56 × 10^7 M^{-1} s^{-1})

(Scheme 2a); thus, the reaction of $SO_4^{\bullet-}$ with 1,2-DHI is expected to contribute to the formation of organosulfates.[8,9]

Scheme 2. Representative Examples of Reactions of the Sulfate Radical[a]

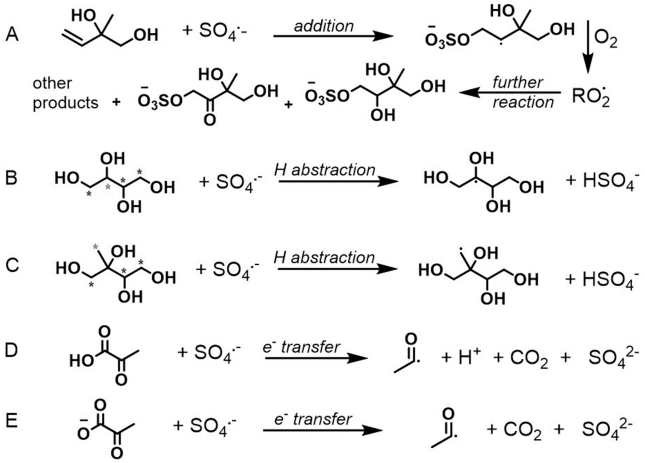

[a](A) The reaction with 1,2-DHI through addition to the double bond, which forms an alkylperoxy radical (RO_2) in the presence of oxygen and eventually stable organosulfate products through RO_2 + RO_2 chemistry and other reactions. (B) H-atom abstraction from erythritol versus (C) 2-methyltetrol, where the blue asterisks denote identical abstraction sites and the magenta asterisks denote different abstraction sites between the two compounds. (D) The direct electron transfer reaction of carboxylic acids and (E) their carboxylates, which results in a decarboxylation reaction that propagates carbon-centered radicals. The reactions shown here do not represent all reactive pathways that may occur for each compound of interest.

The aqueous $SO_4^{\bullet-}$ rate coefficient of 1,2-DHI for this work (1.14 × 10^8 M^{-1} s^{-1}) is comparable to $SO_4^{\bullet-}$ rate coefficients that have been reported for other atmospherically relevant alkenes, such as methacrolein and methylvinylketone (9.9 × 10^7 and 1.1 × 10^8 M^{-1} s^{-1}, respectively).[25] The reaction of MT is ∼30% slower than that of erythritol, which may be rationalized on the basis of their structural differences. MT has the same basic structure as erythritol but has an additional methyl group at the second carbon; thus, MT has a less-

https://doi.org/10.1021/acs.jpca.2c04964
J. Phys. Chem. A 2022, 126, 6517−6525

reactive primary-carbon abstraction site (R-(HO)(C**H**$_3$)C-R) compared to the secondary-carbon abstraction site (R-(HO)**H**C-R) of erythritol (Scheme 2b and c). For the organic dihydroxy dinitrates of isoprene,[33] we expect the major isomer MD-2,3-DN to be formed from gas-phase oxidation. However, once formed and partitioned to the condensed phase, its aqueous oxidation will not be competitive with the fast hydrolysis fate.[46,47] The hydrolysis product formed from MD-2,3-DN, namely, 2-methyl-1,2,4-triol-3-nitrate (MT-3-N), was studied here due to its higher relevance for the aqueous reaction. The mononitrate MT-3-N participated in direct photolysis as well as the $SO_4^{\bullet-}$ reaction, and the corrected rate coefficient ($\sim 3 \times 10^7$ M^{-1} s^{-1}) was similar to that of MT within uncertainty. This could potentially suggest that substitution of an OH group with a ONO_2 group at a secondary carbon does not significantly change the $SO_4^{\bullet-}$ reactivity. As opposed to the major dinitrate MD-2,3-DN, the minor dinitrate isomers (nitrates at the 1,4- and 1,3-positions) are expected to build up in concentration in the condensed phase given their slow hydrolysis fates.[48] Thus, the aqueous oxidation of the minor dinitrate isomers such as MD-1,4-DN would be a competitive fate. However, we found that MD-1,4-DN was relatively slow with respect to its reaction with $SO_4^{\bullet-}$ ($\sim 5 \times 10^6$ M^{-1} s^{-1}). Its reaction with OH radicals is also relatively slow.[27] It is not clear at this time whether this finding is relevant to nitrates in the primary position or whether substitution with two nitrate groups has outsized effects compared to one. Relative to its rate coefficient with aqueous OH ($\sim 2 \times 10^8$ M^{-1} s^{-1}),[27] the $SO_4^{\bullet-}$ reaction of MD-1,4-DN may not be competitive unless the particle phase supplies a large reservoir of sulfate radicals.

We studied the organosulfates as their sodium salts, as the pK_a values of these species are expected to be negative.[49] Both the primary organosulfate, MT-4-S ($\sim 1 \times 10^7$ M^{-1} s^{-1}), and the secondary organosulfate, MD-3-S ($\sim 5 \times 10^6$ M^{-1} s^{-1}), had low reactivities with $SO_4^{\bullet-}$; however, the third OH group in MD-3-S is absent, which does not allow for an exact structural comparison. This is drastically different from the OH rates, where MT-4-S has a k_{OH} rate only 20% slower than that for erythritol. MT-4-S has a faster k_{SO4} than MD-3-S (about two times faster), a trend similar to what we observe with the OH radical. Within organic aerosols of isoprene, the sulfate in the tertiary position is expected to be the major isomer, either from the reaction of the sulfate radical with isoprene[50] or from the ring opening of the isoprene epoxydiols,[51] but the secondary species is also present. The equivalent primary OS has not been observed, although it was studied here due to the enhanced feasibility of its organic synthesis. Unlike the tertiary nitrates of isoprene, the tertiary sulfate is fairly stable with respect to hydrolysis,[52] so oxidation is a competitive fate. It is presumed that the $SO_4^{\bullet-}$ rate of the tertiary sulfate will be within a factor of two or three of the primary sulfate, assuming general substitution trends from OH oxidation can be applied here.[53−58] With this assumption, we can estimate a lower limit of 3.5×10^6 M^{-1} s^{-1} for the tertiary species.

A number of organic acids that have been observed in atmospheric aerosols[59] were investigated in this study. As these acids exist in the environment as either their neutral or anionic forms depending on the pH, two atmospherically relevant pH values were studied: pH 2 for relevance to sulfate-based aerosols and pH 5 for relevance to cloud droplets. In general, we found the k_{SO4} coefficients of the organic acids under study to be slightly lower at pH 2 compared to pH 5 (Figure 5), although in some cases it was challenging to reach this conclusion within uncertainty. This general trend was also observed for other organic acids, with differences between the reaction of the carboxylate and the acid most severe for formic acid (~2 orders of magnitude) and less so for larger acids and diacids (within 10% for malic acid).[60] $SO_4^{\bullet-}$ radicals efficiently decarboxylate carboxylic acids through electron transfer (Scheme 2d and e),[61] and the carboxylate form facilitates this reaction for some compounds.[62] For lactate at pH 5, our k_{SO4} coefficient ($\sim 2 \times 10^7$ M^{-1} s^{-1}) in the range of 293−322 K is in reasonable agreement with a previously determined value ($\sim 1.6 \times 10^7$ M^{-1} s^{-1}) at pH 9, which was controlled at 298 K.[60] Our value for lactic acid at pH 2 ($\sim 1.4 \times 10^7$ M^{-1} s^{-1}) is also within error of the value determined previously ($\sim 1.0 \times 10^7$ M^{-1} s^{-1} at pH 1); discrepancies are likely due to the temperature difference between our study and the cited study. Methylglycerate at pH 5 was found to have a k_{SO4} similar to that of lactate. Both methylglycerate and lactate have one $-CH_2-$ carbon and one $-CH_3$ carbon, so perhaps their similar rate coefficients can be rationalized through structural similarities. Methylglyceric acid (MGA) at pH 2 was originally determined to have a slightly higher rate coefficient than methylglycerate; however, there is possibly a photolysis correction that should be applied. Although MGA did not have a high extinction coefficient at 254 nm (~ 10 M^{-1} cm^{-1}), the possibility for a quantum yield higher than unity could make direct photolysis a concern. We did not have additional MGA samples with which to study the direct photolysis. We applied the same chromophore loss quantum yield for pyruvic acid to estimate a maximum correction due to direct photolysis and found that up to a 15% reduction in k_{SO4} could be expected if MGA behaved like PA with respect to direct photolysis. We do not expect MGA to be quite as photolytically labile as PA as it is missing the carbonyl chromophore of PA. Within error, we conclude that MGA has a rate coefficient similar to methylglycerate. Otto, Schaefer, and Herrmann[26] found a weak pH dependence for the k_{SO4} of terpene-derived organic acids, an observation that also applies to this data set.

The $SO_4^{\bullet-}$ reaction of pyruvate was found to be twice as fast as those of lactate and methylglycerate. The direct photolysis of pyruvate was slow; thus, the correction is fairly minor at pH 5. At pH 2, pyruvic acid (PA) has the fastest direct photolysis rate (Figure S3), which led to a greater than 50% correction to its observed rate of decay. PA appears slower than pyruvate in its $SO_4^{\bullet-}$ reaction after the correction, although this is not clear within uncertainty. It is safe to say, however, that PA reacts faster with $SO_4^{\bullet-}$ than the other studied carboxylic acids. The data here appear to be in good agreement with those of Otto, Schaefer, and Herrmann,[26] who found the k_{SO4} of *cis*-pinonic acid (a keto acid) to be $\sim 3 \times 10^7$ M^{-1} s^{-1} and that of camphoric acid (diacid without the carbonyl group) to be roughly half this value. It is possible that a carbonyl group in the structure of an organic acid increases the rate of reaction with $SO_4^{\bullet-}$ due to the production of an acyl radical (Scheme 2 d and e) compared to an alkyl radical, but this remains to be further explored.

CONCLUSIONS

We reported second-order $SO_4^{\bullet-}$ rate constants for a number of atmospherically relevant compounds (Table 1). Within the studied compounds, we found the alkene 1,2-DHI reacted the fastest with $SO_4^{\bullet-}$ and the dihydroxy (primary) dinitrate MD-

https://doi.org/10.1021/acs.jpca.2c04964
J. Phys. Chem. A 2022, 126, 6517−6525

1,4-DN reacted the slowest, which is similar to their relative reactivities with OH radicals.[27] There are also different trends that may highlight the greater selectivity of $SO_4^{\bullet-}$ reactions; for example, MT-4-S reacted with $SO_4^{\bullet-}$ faster than MT when that trend was reversed with OH. The C_3−C_5 acids under study did not have significantly different reactivities with $SO_4^{\bullet-}$ compared to their carboxylates within the uncertainties of the analyses. Of particular interest may be the reaction of 1,2-DHI with $SO_4^{\bullet-}$, which is able to form surface-active organosulfates,[8−10,50] or the potential reaction of MT-4-S with $SO_4^{\bullet-}$ to propagate sulfur radicals.[21] For other compounds, the k_{SO4} rates determined here may help improve the understanding of aerosol mass loss, which may be underpredicted in current models.[63] However, even with a better understanding of k_{SO4} and k_{OH} rate coefficients, a comparison of $SO_4^{\bullet-}$ versus OH sinks for various organics may still be qualitative at this time. Oxidant concentrations in deliquesced particles and clouds are major sources of uncertainty in multiphase modeling. Models predict a vast range of steady-state OH concentrations in the atmospheric aqueous phase[64] and often overestimate $[OH]_{aq}$ by orders of magnitude compared to measured values that have been reported within quite a narrow range ($(0.1-0.6) \times 10^{-15}$ M for aerosols).[65−67] While revisions of state-of-the-art model mechanisms such as CAPRAM significantly reduce the predicted OH concentrations compared to previous versions,[64] the $SO_4^{\bullet-}$ concentrations in models have not yet been revised, potentially due to the lower amount of available data. Aerosol water $SO_4^{\bullet-}$ concentrations in urban-influenced environments are predicted to be roughly 1×10^{-14} M in the most recent version of CAPRAM. However, there are no measured $SO_4^{\bullet-}$ concentrations in deliquesced aerosols or cloud or fogwater with which to compare these values. If we keep $[SO_4^{\bullet-}]_{aq}$ at 1×10^{-14} M and allow the full range of measured $[OH]_{aq}$ to compete, the $SO_4^{\bullet-}$ reaction would span from 10−70% of the summed reactivity of the organic using kinetic data reported by our group (assuming 2-methyltetrol and 1,2-DHI as the organics). We ignore the reactivity with NO_3 radical for now, as its rate coefficients with the compounds under study have yet not been determined. Thus, there may be situations in mixed urban−biogenic environments (such as regions of the Southeast US) for $SO_4^{\bullet-}$ to be a competitive fate of some organics in aerosols; however, better constraints on aqueous oxidant sources are likely needed in order to improve the understanding of the reactive fates of aerosol-phase compounds.

■ ASSOCIATED CONTENT

Supporting Information

The Supporting Information is available free of charge at https://pubs.acs.org/doi/10.1021/acs.jpca.2c04964.

Kinetic competition calculation between $SO_4^{\bullet-}$ and OH, direct photolysis parameters, photolysis correction calculations, temperature of the reaction medium, magnified view of extinction coefficients, plot of direct photolysis control data, and plot of dark control data (PDF)

■ AUTHOR INFORMATION

Corresponding Author

Tran B. Nguyen − *Department of Environmental Toxicology, University of California Davis, Davis, California 95616, United States;* orcid.org/0000-0001-9206-4359; Email: tbn@ucdavis.edu

Authors

Lillian N. Tran − *Department of Environmental Toxicology, University of California Davis, Davis, California 95616, United States*

Karizza A. Abellar − *Department of Chemistry, University of California Davis, Davis, California 95616, United States*

James D. Cope − *Department of Environmental Toxicology, University of California Davis, Davis, California 95616, United States*

Complete contact information is available at: https://pubs.acs.org/10.1021/acs.jpca.2c04964

Notes

The authors declare no competing financial interest.

Data are publicly available in the Dryad Repository (https://datadryad.org/) under the following DOIs: optical extinction coefficients (10.25338/B83M0M) and relative rate kinetic data (10.25338/B8V34S).

■ ACKNOWLEDGMENTS

We gratefully acknowledge funding from the National Science Foundation Environmental Chemical Sciences Program under CAREER Grant 2046933 and from California Agricultural Experiment Station Grant CAD-ETX-2345-H through the USDA National Institute of Food and Agriculture. Funding for the 400 MHz Advance III was provided by the National Science Foundation (9808183) and the National Institute of Health (ES005707-13 (BACS 60)). We thank The Cort Anastasio group at UC Davis for the use of their fiber spectrophotometer and Dr. Kelvin H. Bates for his general assistance.

■ REFERENCES

(1) Wennberg, P. O.; Bates, K. H.; Crounse, J. D.; Dodson, L. G.; McVay, R. C.; Mertens, L. A.; Nguyen, T. B.; Praske, E.; Schwantes, R. H.; Smarte, M. D.; et al. Gas-phase reactions of isoprene and its major oxidation products. *Chem. Rev.* **2018**, *118* (7), 3337−3390.

(2) Ervens, B.; Turpin, B. J.; Weber, R. J. Secondary organic aerosol formation in cloud droplets and aqueous particles (aqSOA): a review of laboratory, field and model studies. *Atmos. Chem. Phys.* **2011**, *11* (8), 11069−11102.

(3) McNeill, V. F. Aqueous organic chemistry in the atmosphere: Sources and chemical processing of organic aerosols. *Environ. Sci. Technol.* **2015**, *49* (3), 1237−1244.

(4) Herrmann, H.; Hoffmann, D.; Schaefer, T.; Bräuer, P.; Tilgner, A. Tropospheric aqueous-phase free-radical chemistry: Radical sources, spectra, reaction kinetics and prediction tools. *ChemPhysChem* **2010**, *11* (18), 3796−3822.

(5) Herrmann, H.; Schaefer, T.; Tilgner, A.; Styler, S. A.; Weller, C.; Teich, M.; Otto, T. Tropospheric Aqueous-Phase Chemistry: Kinetics, Mechanisms, and Its Coupling to a Changing Gas Phase. *Chem. Rev.* **2015**, *115* (10), 4259−4334.

(6) Wojnárovits, L.; Takács, E. Rate constants of sulfate radical anion reactions with organic molecules: A review. *Chemosphere* **2019**, *220*, 1014−1032.

(7) Schindelka, J.; Iinuma, Y.; Hoffmann, D.; Herrmann, H. Sulfate radical-initiated formation of isoprene-derived organosulfates in atmospheric aerosols. *Faraday Discuss.* **2013**, *165*, 237−259.

(8) Ren, H.; Sedlak, J. A.; Elrod, M. J. General Mechanism for Sulfate Radical Addition to Olefinic Volatile Organic Compounds in Secondary Organic Aerosol. *Environ. Sci. Technol.* **2021**, *55* (3), 1456−1465.

(9) Brüggemann, M.; Xu, R.; Tilgner, A.; Kwong, K. C.; Mutzel, A.; Poon, H. Y.; Otto, T.; Schaefer, T.; Poulain, L.; Chan, M. N.; et al. Organosulfates in Ambient Aerosol: State of Knowledge and Future Research Directions on Formation, Abundance, Fate, and Importance. *Environ. Sci. Technol.* **2020**, *54* (7), 3767−3782.
(10) Van Buren, J.; Cuthbertson, A. A.; Ocasio, D.; Sedlak, D. L. Ubiquitous Production of Organosulfates during Treatment of Organic Contaminants with Sulfate Radicals. *Environ. Sci. Technol. Lett.* **2021**, *8* (7), 574−580.
(11) Estillore, A. D.; Hettiyadura, A. P. S.; Qin, Z.; Leckrone, E.; Wombacher, B.; Humphry, T.; Stone, E. A.; Grassian, V. H. Water Uptake and Hygroscopic Growth of Organosulfate Aerosol. *Environ. Sci. Technol.* **2016**, *50* (8), 4259−4268.
(12) Peng, C.; Razafindrambinina, P. N.; Malek, K. A.; Chen, L.; Wang, W.; Huang, R.-J.; Zhang, Y.; Ding, X.; Ge, M.; Wang, X.; et al. Interactions of organosulfates with water vapor under sub-and supersaturated conditions. *Atmos. Chem. Phys.* **2021**, *21* (9), 7135−7148.
(13) Riva, M.; Da Silva Barbosa, T.; Lin, Y.-H.; Stone, E. A.; Gold, A.; Surratt, J. D. Chemical characterization of organosulfates in secondary organic aerosol derived from the photooxidation of alkanes. *Atmos. Chem. Phys.* **2016**, *16* (17), 11001−11018.
(14) Riva, M.; Tomaz, S.; Cui, T.; Lin, Y.-H.; Perraudin, E.; Gold, A.; Stone, E. A.; Villenave, E.; Surratt, J. D. Evidence for an Unrecognized Secondary Anthropogenic Source of Organosulfates and Sulfonates: Gas-Phase Oxidation of Polycyclic Aromatic Hydrocarbons in the Presence of Sulfate Aerosol. *Environ. Sci. Technol.* **2015**, *49* (11), 6654−6664.
(15) Froyd, K. D.; Murphy, S. M.; Murphy, D. M.; de Gouw, J. A.; Eddingsaas, N. C.; Wennberg, P. O. Contribution of isoprene-derived organosulfates to free tropospheric aerosol mass. *Proc. Nat. Acad. Sci.* **2010**, *107* (50), 21360−21365.
(16) Hatch, L. E.; Creamean, J. M.; Ault, A. P.; Surratt, J. D.; Chan, M. N.; Seinfeld, J. H.; Edgerton, E. S.; Su, Y.; Prather, K. A. Measurements of Isoprene-Derived Organosulfates in Ambient Aerosols by Aerosol Time-of-Flight Mass Spectrometry—Part 2: Temporal Variability and Formation Mechanisms. *Environ. Sci. Technol.* **2011**, *45* (20), 8648−8655.
(17) Surratt, J. D.; Gomez-Gonzalez, Y.; Chan, A. W. H.; Vermeylen, R.; Shahgholi, M.; Kleindienst, T. E.; Edney, E. O.; Offenberg, J. H.; Lewandowski, M.; Jaoui, M.; et al. Organosulfate formation in biogenic secondary organic aerosol. *J. Phys. Chem. A* **2008**, *112* (36), 8345−8378.
(18) Benkelberg, H. J.; Warneck, P. Photodecomposition of iron (III) hydroxo and sulfato complexes in aqueous solution: Wavelength dependence of OH and SO4-quantum yields. *J. Phys. Chem.* **1995**, *99* (14), 5214−5221.
(19) Machulek, A.; Moraes, J. E. F.; Okano, L. T.; Silvério, C. A.; Quina, F. H. Photolysis of ferric ions in the presence of sulfate or chloride ions: implications for the photo-Fenton process. *Photochem. Photobiol. Sci.* **2009**, *8* (7), 985−991.
(20) Cope, J. D.; Bates, K. H.; Tran, L. N.; Abellar, K. A.; Nguyen, T. B. Sulfur radical formation from the tropospheric irradiation of aqueous sulfate aerosols. *Proc. Natl. Acad. Sci. U.S.A.* **2022**, *119* (36), No. e2202857119.
(21) Kwong, K. C.; Chim, M. M.; Davies, J. F.; Wilson, K. R.; Chan, M. N. Importance of sulfate radical anion formation and chemistry in heterogeneous OH oxidation of sodium methyl sulfate, the smallest organosulfate. *Atmos. Chem. Phys.* **2018**, *18* (4), 2809−2820.
(22) Pan, M.; Chen, Z.; Shan, C.; Wang, Y.; Pan, B.; Gao, G. Photochemical activation of seemingly inert SO42- in specific water environments. *Chemosphere* **2019**, *214*, 399−407.
(23) Kong, X.; Castarède, D.; Thomson, E. S.; Boucly, A.; Artiglia, L.; Ammann, M.; Gladich, I.; Pettersson, J. B. C. A surface-promoted redox reaction occurs spontaneously on solvating inorganic aerosol surfaces. *Science* **2021**, *374* (6568), 747−752.
(24) Herrmann, H.; Hoffmann, D.; Schaefer, T.; Bräuer, P.; Tilgner, A. Tropospheric Aqueous-Phase Free-Radical Chemistry: Radical Sources, Spectra, Reaction Kinetics and Prediction Tools. *ChemPhysChem* **2010**, *11* (18), 3796−3822.
(25) Schöne, L.; Schindelka, J.; Szeremeta, E.; Schaefer, T.; Hoffmann, D.; Rudzinski, K. J.; Szmigielski, R.; Herrmann, H. Atmospheric aqueous phase radical chemistry of the isoprene oxidation products methacrolein, methyl vinyl ketone, methacrylic acid and acrylic acid - kinetics and product studies. *Phys. Chem. Chem. Phys.* **2014**, *16* (13), 6257−6272.
(26) Otto, T.; Schaefer, T.; Herrmann, H. Aqueous-Phase Oxidation of Terpene-Derived Acids by Atmospherically Relevant Radicals. *J. Phys. Chem. A* **2018**, *122* (47), 9233−9241.
(27) Abellar, K. A.; Cope, J. D.; Nguyen, T. B. Second-Order Kinetic Rate Coefficients for the Aqueous-Phase Hydroxyl Radical (OH) Oxidation of Isoprene-Derived Secondary Organic Aerosol Compounds at 298 K. *Environ. Sci. Technol.* **2021**, *55* (20), 13728−13736.
(28) Hughes, D. D.; Christiansen, M. B.; Milani, A.; Vermeuel, M. P.; Novak, G. A.; Alwe, H. D.; Dickens, A. F.; Pierce, R. B.; Millet, D. B.; Bertram, T. H.; et al. PM2. 5 chemistry, organosulfates, and secondary organic aerosol during the 2017 Lake Michigan Ozone Study. *Atmos. Environ.* **2021**, *244*, 117939.
(29) Claeys, M.; Graham, B.; Vas, G.; Wang, W.; Vermeylen, R.; Pashynska, V.; Cafmeyer, J.; Guyon, P.; Andreae, M. O.; Artaxo, P.; Maenhaut, W. Formation of secondary organic aerosols through photooxidation of isoprene. *Science* **2004**, *303* (5661), 1173−1176.
(30) Clements, A. L.; Seinfeld, J. H. Detection and quantification of 2-methyltetrols in ambient aerosol in the southeastern United States. *Atmos. Environ.* **2007**, *41* (9), 1825−1830.
(31) Karambelas, A.; Pye, H. O.; Budisulistiorini, S. H.; Surratt, J. D.; Pinder, R. W. Contribution of isoprene epoxydiol to urban organic aerosol: evidence from modeling and measurements. *Environ. Sci. Technol. Lett.* **2014**, *1* (6), 278−283.
(32) Chan, M. N.; Surratt, J. D.; Claeys, M.; Edgerton, E. S.; Tanner, R. L.; Shaw, S. L.; Zheng, M.; Knipping, E. M.; Eddingsaas, N. C.; Wennberg, P. O.; et al. Characterization and Quantification of Isoprene-Derived Epoxydiols in Ambient Aerosol in the Southeastern United States. *Environ. Sci. Technol.* **2010**, *44* (12), 4590−4596.
(33) Lee, L.; Teng, A. P.; Wennberg, P. O.; Crounse, J. D.; Cohen, R. C. On rates and mechanisms of OH and O3 Reactions with isoprene-derived hydroxy nitrates. *J. Phys. Chem. A* **2014**, *118*, 1622−1637.
(34) Kjaergaard, H. G.; Knap, H. C.; Ørnsø, K. B.; Jørgensen, S.; Crounse, J. D.; Paulot, F.; Wennberg, P. O. Atmospheric Fate of Methacrolein. 2. Formation of Lactone and Implications for Organic Aerosol Production. *J. Phys. Chem. A* **2012**, *116* (24), 5763−5768.
(35) Nguyen, T. B.; Bates, K. H.; Crounse, J. D.; Schwantes, R. H.; Zhang, X.; Kjaergaard, H. G.; Surratt, J. D.; Lin, P.; Laskin, A.; Seinfeld, J. H.; et al. Mechanism of the hydroxyl radical oxidation of methacryloyl peroxynitrate (MPAN) and its pathway toward secondary organic aerosol formation in the atmosphere. *Phys. Chem. Chem. Phys.* **2015**, *17* (27), 17914−17926.
(36) Chebbi, A.; Carlier, P. Carboxylic acids in the troposphere, occurrence, sources, and sinks: A review. *Atmos. Environ.* **1996**, *30* (24), 4233−4249.
(37) Bondy, A. L.; Craig, R. L.; Zhang, Z.; Gold, A.; Surratt, J. D.; Ault, A. P. Isoprene-Derived Organosulfates: Vibrational Mode Analysis by Raman Spectroscopy, Acidity-Dependent Spectral Modes, and Observation in Individual Atmospheric Particles. *J. Phys. Chem. A* **2018**, *122* (1), 303−315.
(38) Zhu, L.; Nicovich, J. M.; Wine, P. H. Temperature-dependent kinetics studies of aqueous phase reactions of SO4- radicals with dimethylsulfoxide, dimethylsulfone, and methanesulfonate. *J. Photochem. Photobiol., A* **2003**, *157* (2), 311−319.
(39) Nishino, N.; Arey, J.; Atkinson, R. Rate Constants for the Gas-Phase Reactions of OH Radicals with a Series of C6-C14 Alkenes at 299 ± 2 K. *J. Phys. Chem. A* **2009**, *113* (5), 852−857.
(40) Hoffmann, D.; Weigert, B.; Barzaghi, P.; Herrmann, H. Reactivity of poly-alcohols towards OH, NO3 and SO4- in aqueous solution. *Phys. Chem. Chem. Phys.* **2009**, *11* (41), 9351−9363.

https://doi.org/10.1021/acs.jpca.2c04964
J. Phys. Chem. A 2022, 126, 6517−6525

(41) Tang, Y.; Thorn, R. P.; Mauldin, R. L.; Wine, P. H. Kinetics and spectroscopy of the SO4- radical in aqueous solution. *J. Photochem. Photobiol., A* **1988**, *44* (3), 243−258.
(42) Kuhn, H.; Braslavsky, S.; Schmidt, R. Chemical actinometry (IUPAC technical report). *Pure Appl. Chem.* **2004**, *76* (12), 2105−2146.
(43) Compernolle, S.; Müller, J.-F. Henry's law constants of polyols. *Atmos. Chem. Phys.* **2014**, *14* (23), 12815−12837.
(44) Eugene, A. J.; Guzman, M. I. Reactivity of ketyl and acetyl radicals from direct solar actinic photolysis of aqueous pyruvic acid. *J. Phys. Chem. A* **2017**, *121* (15), 2924−2935.
(45) Leermakers, P. A.; Vesley, G. F. The photochemistry of α-keto acids and α-keto esters. I., Photolysis of pyruvic acid and benzoylformic acid. *J. Am. Chem. Soc.* **1963**, *85* (23), 3776−3779.
(46) Zare, A.; Fahey, K. M.; Sarwar, G.; Cohen, R. C.; Pye, H. O. Vapor-pressure pathways initiate but hydrolysis products dominate the aerosol estimated from organic nitrates. *ACS Earth Space Chem.* **2019**, *3* (8), 1426−1437.
(47) Vasquez, K. T.; Crounse, J. D.; Schulze, B. C.; Bates, K. H.; Teng, A. P.; Xu, L.; Allen, H. M.; Wennberg, P. O. Rapid hydrolysis of tertiary isoprene nitrate efficiently removes NOx from the atmosphere. *Proc. Nat. Acad. Sci.* **2020**, *117* (52), 33011−33016.
(48) Hu, K. S.; Darer, A. I.; Elrod, M. J. Thermodynamics and kinetics of the hydrolysis of atmospherically relevant organonitrates and organosulfates. *Atmos. Chem. Phys.* **2011**, *11* (16), 8307−8320.
(49) Hyttinen, N.; Elm, J.; Malila, J.; Calderón, S. M.; Prisle, N. L. Thermodynamic properties of isoprene- and monoterpene-derived organosulfates estimated with COSMOtherm. *Atmos. Chem. Phys.* **2020**, *20* (9), 5679−5696.
(50) Nozière, B.; Ekström, S.; Alsberg, T.; Holmström, S. Radical-initiated formation of organosulfates and surfactants in atmospheric aerosols. *Geophys. Res. Lett.* **2010**, *37* (5), L05806.
(51) Eddingsaas, N. C.; VanderVelde, D. G.; Wennberg, P. O. Kinetics and products of the acid-catalyzed ring-opening of atmospherically relevant butyl epoxy alcohols. *J. Phys. Chem. A* **2010**, *114* (31), 8106−8113.
(52) Darer, A. I.; Cole-Filipiak, N. C.; O'Connor, A. E.; Elrod, M. J. Formation and stability of atmospherically relevant isoprene-derived organosulfates and organonitrates. *Environ. Sci. Technol.* **2011**, *45* (5), 1895−1902.
(53) Thüner, L. P.; Bardini, P.; Rea, G. J.; Wenger, J. C. Kinetics of the gas-phase reactions of OH and NO3 radicals with dimethylphenols. *J. Phys. Chem. A* **2004**, *108* (50), 11019−11025.
(54) Coeur-Tourneur, C.; Cassez, A.; Wenger, J. C. Rate Coefficients for the Gas-Phase Reaction of Hydroxyl Radicals with 2-Methoxyphenol (Guaiacol) and Related Compounds. *J. Phys. Chem. A* **2010**, *114* (43), 11645−11650.
(55) Coeur-Tourneur, C.; Henry, F.; Janquin, M. A.; Brutier, L. Gas-phase reaction of hydroxyl radicals with m-, o-and p-cresol. *Int. J. Chem. Kinet.* **2006**, *38* (9), 553−562.
(56) Olariu, R.; Bejan, I.; Barnes, I.; Klotz, B.; Becker, K.; Wirtz, K. Rate coefficients for the gas-phase reaction of NO3 radicals with selected dihydroxybenzenes. *Int. J. Chem. Kinet.* **2004**, *36* (11), 577−583.
(57) Wang, Y. n.; Chen, J.; Li, X.; Zhang, S.; Qiao, X. Estimation of aqueous-phase reaction rate constants of hydroxyl radical with phenols, alkanes and alcohols. *QSAR Comb. Sci.* **2009**, *28* (11−12), 1309−1316.
(58) Suarez-Bertoa, R.; Picquet-Varrault, B.; Tamas, W.; Pangui, E.; Doussin, J. Atmospheric fate of a series of carbonyl nitrates: photolysis frequencies and OH-oxidation rate constants. *Environ. Sci. Technol.* **2012**, *46* (22), 12502−12509.
(59) Fisseha, R.; Dommen, J.; Sax, M.; Paulsen, D.; Kalberer, M.; Maurer, R.; Höfler, F.; Weingartner, E.; Baltensperger, U. Identification of Organic Acids in Secondary Organic Aerosol and the Corresponding Gas Phase from Chamber Experiments. *Anal. Chem.* **2004**, *76* (22), 6535−6540.
(60) Grgić, I.; Podkrajšek, B.; Barzaghi, P.; Herrmann, H. Scavenging of SO4- radical anions by mono-and dicarboxylic acids in the Mn (II)-catalyzed S (IV) oxidation in aqueous solution. *Atmos. Environ.* **2007**, *41* (39), 9187−9194.
(61) Madhavan, V.; Levanon, H.; Neta, P. Decarboxylation by SO4.- radicals. *Radiat. Res.* **1978**, *76* (1), 15−22.
(62) Luo, S.; Wei, Z.; Dionysiou, D. D.; Spinney, R.; Hu, W.-P.; Chai, L.; Yang, Z.; Ye, T.; Xiao, R. Mechanistic insight into reactivity of sulfate radical with aromatic contaminants through single-electron transfer pathway. *Chem. Eng. J.* **2017**, *327*, 1056−1065.
(63) Bates, K. H.; Jacob, D. J. A new model mechanism for atmospheric oxidation of isoprene: global effects on oxidants, nitrogen oxides, organic products, and secondary organic aerosol. *Atmops. Chem. Phys.* **2019**, *19* (14), 9613−9640.
(64) Tilgner, A.; Herrmann, H., Tropospheric Aqueous-Phase OH Oxidation Chemistry: Current Understanding, Uptake of Highly Oxidized Organics and Its Effects. In *Multiphase Environmental Chemistry in the Atmosphere*; Hunt, S. W., Laskin, A., Nizkorodov, S. A., Eds.; ACS Symposium Series, Vol. *1299*; ACS Publications: Washington, D.C., 2018; pp 49−85.
(65) Kaur, R.; Anastasio, C. Light absorption and the photoformation of hydroxyl radical and singlet oxygen in fog waters. *Atmos. Environ.* **2017**, *164*, 387−397.
(66) Anastasio, C.; McGregor, K. G. Chemistry of fog waters in California's Central Valley: 1. In situ photoformation of hydroxyl radical and singlet molecular oxygen. *Atmos. Environ.* **2001**, *35* (6), 1079−1089.
(67) Arakaki, T.; Anastasio, C.; Kuroki, Y.; Nakajima, H.; Okada, K.; Kotani, Y.; Handa, D.; Azechi, S.; Kimura, T.; Tsuhako, A.; et al. A General Scavenging Rate Constant for Reaction of Hydroxyl Radical with Organic Carbon in Atmospheric Waters. *Environ. Sci. Technol.* **2013**, *47* (15), 8196−8203.

https://doi.org/10.1021/acs.jpca.2c04964
J. Phys. Chem. A 2022, 126, 6517−6525